Effects of hydrostatic pressure and aluminum concentration on the conduction-electron *g* factor in GaAs-(Ga,Al)As quantum wells under in-plane magnetic fields

E. Reyes-Gómez and N. Raigoza
Instituto de Física, Universidad de Antioquia, AA 1226 Medellín, Colombia

L. E. Oliveira
Instituto de Física, Unicamp, Caixa Postal 6165, Campinas, São Paulo 13083-970, Brazil
(Received 24 November 2007; published 10 March 2008)

The effects of hydrostatic pressure and aluminum concentration on the conduction-electron effective Landé *g* factor in semiconductor GaAs-$Ga_{1-x}Al_xAs$ quantum wells under in-plane magnetic fields are presented. Numerical calculations of the conduction-electron Landé *g* factor are performed by taking into account the nonparabolicity and anisotropy of the conduction band via the Ogg–McCombe Hamiltonian as well as the effects of aluminum concentration and applied hydrostatic pressure. Theoretical results are given as functions of the aluminum concentration in the $Ga_{1-x}Al_xAs$ barrier, orbit-center position, applied in-plane magnetic field, hydrostatic pressure, and quantum-well width, and found in good agreement with experimental measurements in GaAs-$Ga_{1-x}Al_xAs$ quantum wells for various values of the aluminum concentration *x* in the absence of hydrostatic pressure.

DOI: 10.1103/PhysRevB.77.115308 PACS number(s): 73.21.Fg, 71.18.+y, 78.55.Cr

I. INTRODUCTION

In semiconductors and its heterostructures, the electron Landé *g* factor determines the spin splitting of carrier bands and influences the spin dynamics and spin resonance in such materials. Therefore, there has been a number of experimental and theoretical work devoted to the understanding of the properties of the electron effective *g* factor in such semiconductor systems.[1–14] Due to the potential applications in the design and fabrication of spintronic and optoelectronic devices,[15–17] such studies have been focused in semiconductor-bulk materials,[1–4] quantum wells (QWs),[5–11] quantum-well wires,[12] quantum dots,[13] and superlattices.[14]

Since the pioneering work of Weisbuch and Hermann,[1,2] the properties of the electron *g* factor in bulk $Ga_{1-x}Al_xAs$ have received great attention. For example, Oestreich and co-workers[3,4] studied the temperature dependence of the frequency of quantum beats of the free electron Larmor precession in GaAs bulk and obtained a growing *g* factor as a function of the temperature. Also, the electron *g* factor was measured, in QWs, by Hannak *et al.*,[5] Le Jeune *et al.*,[6] Malinowski and Harley,[7] Heberle *et al.*,[8] and more recently by Yugova *et al.*,[9] who found that the component of the electron *g* factor along the growth axis, as a function of the electron-transition energy, follows an universal behavior. From the theoretical point of view, however, investigations on the properties of the effective Landé *g* factor in QWs have been mainly carried out without the consideration of hydrostatic-pressure effects, which have proven to be of great value in the study of skyrmions in the limit of zero *g* factor.[18] In III-V bulk materials, the properties of the electron Landé *g* factor may be investigated within the $\mathbf{k}\cdot\mathbf{p}$ framework.[1–4,9] According to this procedure, the behavior of the Landé *g* factor in $Ga_{1-x}Al_xAs$, as a function of hydrostatic pressure (P) and aluminum concentration (x), is determined by the dependency of the fundamental gaps[19–24] and interband transition-matrix elements[9] as functions of P and x. In a QW, however, the electron Landé factor must be studied by taking into account the barrier-confinement effects on the electron localization properties as well as the anisotropy and nonparabolicity of the conduction band. In that respect, the effective Ogg–McCombe Hamiltonian[25,26] has been successfully used in order to obtain the effective Landé factor in GaAs-$Ga_{1-x}Al_xAs$ QWs.[10,11] The aim of the present work is to study the hydrostatic pressure and aluminum concentration effects on the electron *g* factor in GaAs-$Ga_{1-x}Al_xAs$ QWs under in-plane magnetic fields by taking into account the anisotropy and nonparabolicity of the conduction band. The paper is organized as follows. The theoretical procedure and a discussion of the effects of hydrostatic pressure and aluminum concentration on the *g* factor in bulk $Ga_{1-x}Al_xAs$ and GaAs-$Ga_{1-x}Al_xAs$ QW confining potential are given in Sec. II. Results and discussions are in Sec. III, and conclusions in Sec. IV.

II. THEORETICAL FRAMEWORK

In the effective-mass approximation and taking into account the nonparabolicity and anisotropy effects on the conduction band, the Ogg–McCombe effective Hamiltonian[25,26] for a conduction-electron in a GaAs-$Ga_{1-x}Al_xAs$ QW grown along the y axis, under an in-plane $\mathbf{B}=B\hat{\mathbf{z}}$ magnetic field and applied hydrostatic pressure, may be written as

$$\hat{H}=\frac{\hbar^2}{2}\hat{\mathbf{K}}\frac{1}{m(x,P,y)}\hat{\mathbf{K}}+\frac{1}{2}g(x,P,y)\mu_B\hat{\sigma}_z B+a_1\hat{\mathbf{K}}^4+\frac{a_2}{l_B^4}+a_3[\{\hat{K}_x^2,\hat{K}_y^2\}+\{\hat{K}_x^2,\hat{K}_z^2\}+\{\hat{K}_y^2,\hat{K}_z^2\}]+a_4B\hat{\mathbf{K}}^2\hat{\sigma}_z+a_5\{\hat{\boldsymbol{\sigma}}\cdot\hat{\mathbf{K}},\hat{K}_zB\}+a_6B\hat{\sigma}_z\hat{K}_z^2+V(x,P,y), \quad (1)$$

where $\hat{\mathbf{K}}=-i\nabla+\frac{e}{\hbar c}\hat{\mathbf{A}}$ is the generalized momentum operator, $\hat{\mathbf{A}}$ is the magnetic vector potential, $\hat{\boldsymbol{\sigma}}$ is a vector with Pauli matrices as components, μ_B is the Bohr magneton, $l_B=\sqrt{\frac{\hbar c}{eB}}$ is

 ©2008 The American Physical Society

the Landau length, $\{\hat{a},\hat{b}\}=\hat{a}\hat{b}+\hat{b}\hat{a}$ is the anticommutator between the $\hat{a}$ and $\hat{b}$ operators, and the coefficients a_1, a_2, a_3, a_4, a_5, and a_6 are constants which depend, in principle, on the aluminum concentration x and applied hydrostatic pressure P. Due to the absence of experimental measurements on the behavior of the a_i coefficients as functions of P and x, we have taken the a_i values corresponding to bulk GaAs and obtained by a fitting with magnetospectroscopic measurements.[27] Recent work has used this set of parameters in order to study the electron spin relaxation in n-type semiconductors.[28] Here, we have ignored the Dresselhaus cubic spin-orbit interaction[29] as its contribution to the effective g factor in GaAs-(Ga,Al)As heterostructures may be shown to be quite minor.[30] The growth-direction position-dependent conduction-electron effective mass $m(x,P,y)$ and Landé factor $g(x,P,y)$, together with the electron-confining potential $V(x,P,y)$, are considered to be dependent on the applied hydrostatic pressure and aluminum concentration in the $Ga_{1-x}Al_xAs$ barrier of the heterostructure, as detailed below.

The eigenfunctions of Eq. (1) may be chosen as

$$\Psi(\mathbf{r}) = \frac{e^{i(xk_x+zk_z)}}{\sqrt{S}}\sum_n \begin{bmatrix} C_{n\uparrow} \\ C_{n\downarrow} \end{bmatrix} |n,y_0\rangle, \quad (2)$$

where $|n,y_0\rangle$ are the harmonic-oscillator wave functions, k_x and k_z are the in-plane components of the electron wave vector, and $y_0=k_x l_B^2$ is the cyclotron orbit-center position. At low temperatures, one may disregard the k_z energy dependence, i.e., one takes $k_z=0$, the states with different spin projections (parallel ↑ or antiparallel ↓) along the magnetic-field direction are uncoupled, and the Schrödinger equation,

$$\sum_n \left(\begin{bmatrix} H_{0\uparrow}^{mn} & 0 \\ 0 & H_{0\downarrow}^{mn} \end{bmatrix} - E \begin{bmatrix} 1 & 0 \\ 0 & 1 \end{bmatrix} \delta_{mn} \right) \begin{bmatrix} C_{n\uparrow} \\ C_{n\downarrow} \end{bmatrix} = 0, \quad (3)$$

written in the harmonic-oscillator representation, may be readily solved.[10,14] The effective Landé $g_\perp^{(n)}$ factor in the in-plane direction (perpendicular to the y-growth axis) in GaAs-(Ga,Al)As heterostructures may therefore be defined as

$$g_\perp^{(n)} = \frac{E_{n\uparrow} - E_{n\downarrow}}{\mu_B B}, \quad (4)$$

where $E_{n\uparrow}$ and $E_{n\downarrow}$ are the energies associated with the spin-up and spin-down Landau levels, respectively, and μ_B is the Bohr magneton. The effective $g_\perp^{(n)}$ factor, obtained from Eq. (4), depends on the hydrostatic pressure, aluminum concentration in the $Ga_{1-x}Al_xAs$ barriers, applied magnetic field, and orbit-center position.

A. Electron g factor and effective mass in $Ga_{1-x}Al_xAs$

In order to compute the effective Landé factor in GaAs-(Ga,Al)As heterostructures from Eq. (4), one needs to know the dependence of both the electron g factor and effective mass on the applied hydrostatic pressure in each QW material. In that respect, one may resort to the $\mathbf{k}\cdot\mathbf{p}$ perturbation theory, which has proven of great value in the calculation of many electrical and optical properties of a large number of systems. According to the $\mathbf{k}\cdot\mathbf{p}$ procedure, the electron Landé g factor and effective mass in a III-V material are given by[2,9]

$$g = g_0\left[1 - \frac{\Pi^2}{3}\frac{\Delta_0}{E_g^\Gamma[E_g^\Gamma + \Delta_0]} + \delta_g\right] \quad (5)$$

and

$$m = m_0\left[1 + \frac{\Pi^2}{3}\left(\frac{2}{E_g^\Gamma} + \frac{1}{E_g^\Gamma + \Delta_0}\right) + \delta_m\right]^{-1}, \quad (6)$$

respectively, where $g_0=2.0023$ and m_0 are the free-electron Landé factor and effective mass, respectively, $\Pi^2 = \frac{2}{m_0}|\langle S|\hat{p}_x|X(\Gamma_5^v)\rangle|^2$ is the square of the interband matrix element describing the coupling between the s states of the Γ_6^c conduction band with the hybrid sp-valence states corresponding to Γ_8^v and Γ_7^v (Γ_5^v), $E_g^\Gamma=E(\Gamma_6^c)-E(\Gamma_8^v)$ is the fundamental gap, and $\Delta_0=E(\Gamma_8^v)-E(\Gamma_7^v)$ is the split-off valence gap. The remote-band effects on the electron Landé factor and the effective mass are taken into account via δ_g and δ_m, respectively, which are essentially dominated by the energy differences $E'=E(\Gamma_8^c)-E_g^\Gamma$ and $E''=E(\Gamma_7^c)-E_g^\Gamma$, and by the interband matrix elements $\Pi'^2=\frac{2}{m_0}|\langle S|\hat{p}_x|X(\Gamma_5^c)\rangle|^2$ (see Ref. 2 for details). The effects of the applied hydrostatic pressure and aluminum concentration on the electron g factor and effective mass corresponding to a given III-V compound are taken into account via the hydrostatic-pressure and aluminum concentration dependencies of the different energy gaps and interband matrix elements in each material. We have denoted by $E(P,x)$ the energies involved in Eqs. (5) and (6), as well as the X-point energy of the conduction band (measured with respect to the top of the valence band) $E_g^X = E(X_6^c)-E(\Gamma_8^v)$, and assume that

$$E(x,P) = a + bx + cx^2 + \alpha(x)P. \quad (7)$$

The values of a, b, c, and $\alpha(x)$ corresponding to $Ga_{1-x}Al_xAs$ are displayed in Table I. The remote-band contributions to the electron g factor and effective mass are also expected to be functions of the applied hydrostatic pressure and aluminum concentration. However, up to now we do not know of any experimental report on such dependencies in $Ga_{1-x}Al_xAs$ bulk materials. We have, therefore, considered δ_g and δ_m in Eqs. (5) and (6), respectively, depending only on the aluminum x concentration according to the expression

$$\delta(x) = \delta_0 + \delta_1 x + \delta_2 x^2, \quad (8)$$

with the values of δ_0, δ_1, and δ_2, reported in Table II, chosen in order to fit the experimental results corresponding to the electron g factor[2] and effective mass[31] at $P=0$ [cf., Fig. 2].

B. Pressure-dependent GaAs-$Ga_{1-x}Al_xAs$ quantum well confining potential

It is well known that effects of applied hydrostatic pressure modify the semiconductor band structure and lead to changes in the properties of elementary excitations in semiconductor heterostructures. As the hydrostatic pressure increases, a crossover between the Γ and X conduction-band minima takes place. The pressure dependence of the

TABLE I. Parameters used in the present calculation.

$E(x,P)$	a (eV)	b (eV)	c (eV)	$\alpha(x)$ (meV/kbar)
E_g^Γ	1.5194[a]	1.36[a]	0.22[a]	10.7[b]
Δ_0	0.341[c]	−0.066[c]	0[c]	0[d]
Π^2	28.90[e]	−6.29[f]	0[f]	0[g]
E_g^X	1.988[h]	0.207[h]	0.055[h]	−1.35[i]

[a]From Ref. 19.
[b]From Ref. 20.
[c]From Ref. 21.
[d]From Ref. 22.
[e]From Refs. 2 and 9.
[f]Obtained from a linear fitting of the Π^2 values for bulk $Ga_{1-x}Al_xAs$, reported in Ref. 9.
[g]To our knowledge, there are no experimental measurements on the hydrostatic-pressure dependence of the Π^2 matrix element, so we have taken $\alpha(x)=0$.
[h]From Ref. 23.
[i]From Ref. 24 for GaAs. We have assumed that the Γ-X pressure coefficient in $Ga_{1-x}Al_xAs$ does not depend on the aluminum concentration.

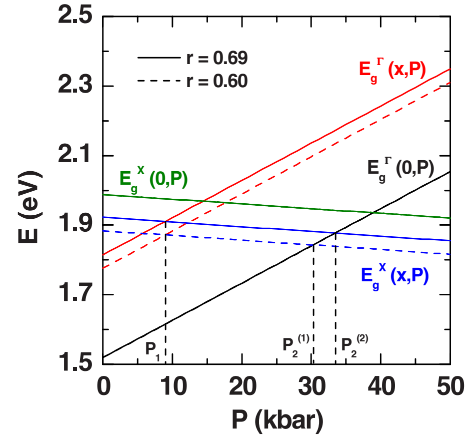

FIG. 1. (Color online) Relative position of the conduction-band minima Γ and X both in GaAs and $Ga_{0.7}Al_{0.3}As$ as functions of applied hydrostatic pressure. The origin of the energies was taken at the top of the GaAs valence band. Calculations were carried out for two different values of the height of the conduction-confining potential, obtained by using two different r fractions of the band-gap discontinuity.

electron-confining potential in a GaAs-$Ga_{1-x}Al_xAs$ QW is determined by two critical values P_1 and P_2 of the hydrostatic pressure, corresponding to the crossing between the Γ and X points at the $Ga_{1-x}Al_xAs$ barriers [with energies $E_g^\Gamma(x,P)$ and $E_g^X(x,P)$, respectively], and to the crossing between the Γ point at the GaAs well [with energy $E_g^\Gamma(0,P)$] and the X point at the barriers, respectively. For $P<P_1$, the height of the electron-confining potential is considered to be independent of the applied hydrostatic pressure and obtained as a fraction r of the difference between the $Ga_{1-x}Al_xAs$ and GaAs energy gaps at the Γ point. This is the so-called direct-gap regime. For $P_1<P<P_2$, the X minima fall below the Γ minima in the barrier layers. Therefore, the height of the confining potential decreases as the hydrostatic pressure is increased and is proportional to a fraction r of the energy difference $E_g^X(x,P)-E_g^\Gamma(0,P)+S_{\Gamma X}(x,P)$, where

$$S_{\Gamma X}(x,P)=S_0\frac{P-P_1}{P}x \tag{9}$$

is the pressure-dependent Γ-X mixing strength coefficient, with $S_0=250$ meV being an adjustable parameter which fits the experimental measurements.[32] In this case, it is said that the system is in the indirect-gap regime. For $P>P_2$, the X point at the barriers becomes the absolute minimum of the conduction band, and a type I–type II transition is expected to occur in the semiconductor heterostructure.

The value of the aluminum concentration at the barriers may also dramatically change the properties of the confining potential. As it is well known, there exists a critical value x_c of the aluminum concentration at which the Γ-X crossover takes place in the barriers. At low temperatures and in the absence of applied hydrostatic pressure, the value $x_c=0.385$ was found by Guzzi *et al.*[23] In addition, the critical values P_1 and P_2 also depend on the concentration x at the barriers. Here, we shall only consider hydrostatic-pressure values between zero and P_2, and aluminum concentrations between zero and x_c.

The above considerations may be summarized in Fig. 1, where we have shown the behaviors of E_g^Γ and E_g^X both in bulk GaAs and $Ga_{1-x}Al_xAs$, according to the values displayed in Table I, as functions of the applied hydrostatic pressure. The origin of the energies is taken at the top of the GaAs valence band. We have considered two different values of the r parameter: $r=0.6$ as in Ref. 10 and $r=0.69$ as in Ref. 33. One may note that the value of P_1 does not depend on r, whereas two values of P_2 were obtained for each value of r (a fact which may be used to experimentally find the appropriate r value). This model was successfully used in the study of shallow-impurity states in single QWs[32] and electron states in double-coupled and multiple uncoupled QW heterostructures[33] under hydrostatic pressure. For our purposes, we shall use in the next section the value $r=0.6$ as in Ref. 10.

For $P\leqslant P_2$ applied hydrostatic pressure, the electron-confining potential is therefore given by[32]

$$V(x,P,y)=\begin{cases} V_0(x,P) & \text{if } |y|>\dfrac{L(P)}{2} \\ 0 & \text{if } |y|\leqslant\dfrac{L(P)}{2}, \end{cases} \tag{10}$$

with

TABLE II. Aluminum x concentration dependence of the remote-band contributions for the electron g factor and effective mass of bulk $Ga_{1-x}Al_xAs$ at $P=0$.

$\delta(x)$	δ_0	δ_1	δ_2
δ_g	−0.056	−0.276	0.232
δ_m	−3.935	0.488	4.938

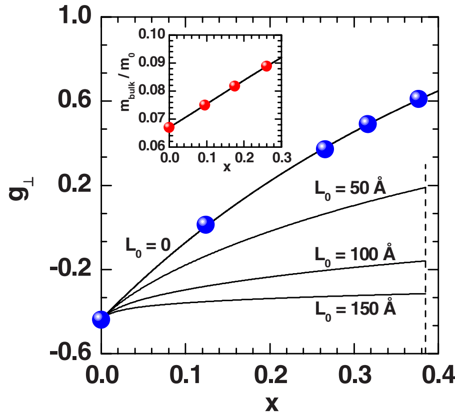

FIG. 2. (Color online) Effective $g_\perp$ factor as a function of the concentration x in GaAs-$Ga_{1-x}Al_xAs$ QWs under an in-plane magnetic field $B=1$ T for the orbit-center position at the center of the wells. Theoretical results for $L_0=0$ were obtained for $B=0$ according to expression (5). Solid symbols correspond to the experimental measurements reported by Hermann and Weisbuch (Ref. 2) in the absence of the applied magnetic field. Results in the inset correspond to the x dependence of the electron-effective mass in bulk $Ga_{1-x}Al_xAs$ at $B=0$, obtained from expression (6). Solid symbols in the inset correspond to the experimental results by Zachau *et al.* (Ref. 31).

$$V_0(x,P) = r\begin{cases} E_g^\Gamma(x,P) - E_g^\Gamma(0,P) & \text{if } 0 < P \leq P_1 \\ E_g^X(x,P) - E_g^\Gamma(0,P) + S_{\Gamma X}(x,P) & \text{if } P_1 < P \leq P_2. \end{cases} \quad (11)$$

The pressure-dependent QW width in expression (10) is given by $L(P)=L_0[1-(S_{11}+2S_{12})P]$, where L_0 is the well width in the absence of applied hydrostatic pressure and S_{11} and S_{12} are the compliance constants[34] of bulk GaAs.

III. RESULTS AND DISCUSSION

We have first calculated the effective Landé $g_\perp$ factor in GaAs-$Ga_{1-x}Al_xAs$ QWs as a function of the x concentration in the absence of the hydrostatic pressure. Theoretical results are displayed in Fig. 2 for various values of the well width. The dashed vertical line in the figure corresponds to the x_c limit reported by Guzzi *et al.*[23] Calculations for $L_0=0$ (bulk $Ga_{1-x}Al_xAs$ at $B=0$) were performed by using expression (5) and compared with experimental data for the effective g factors reported by Hermann and Weisbuch.[2] Experimental values of the electron-effective mass as a function of x are also displayed (see inset of Fig. 2) together with the numerical results obtained from Eq. (6) for $B=0$ and in the absence of applied hydrostatic pressure. The appropriated choice of the δ parameters in Table II guarantees the excellent agreement between theoretical calculations and experimental measurements in both cases. In addition, the fitting for the electron effective mass agrees with the linear fitting $m=m_0(0.067+0.083x)$ reported by Adachi.[35] It is apparent from Fig. 2 that the electron $g_\perp$ factor increases with the aluminum concentration in the barriers, although changes are less dramatic as the well width is increased. For small values of the QW width, the electron wave function has a larger penetration in the barrier regions, and therefore, the effective $g_\perp$ factor is strongly influenced by the barriers properties. On the other hand, as the well width is increased, the electron wave function does not "feel" much of the $Ga_{1-x}Al_xAs$ barrier potential, and the effective $g_\perp$ factor becomes essentially independent of the aluminum concentration at the QW barriers. Results shown in Fig. 2 were obtained for the orbit-center position at the center of the well. The effective Landé factor is a function of the orbit-center position y_0, and such dependence is displayed in Fig. 3 for a GaAs-$Ga_{0.7}Al_{0.3}As$ QW with $L_0=50$ Å and for three different values of the applied hydrostatic pressure. For $B=1$ T, the ground-state electron-localization magnetic length $l_B \gg L$ in the whole range of the hydrostatic pressure considered in the present study, the spin-up and spin-down electron energies are essentially flat as functions of the orbit-center position, and therefore, the $g_\perp$ factor weakly depends on y_0. For $B=20$ T, however, we have $l_B \sim L$ and electron energies as well as the $g_\perp$ factor become dispersive as functions of the orbit-center position. As a result, at low temperatures and small values of the applied in-plane magnetic field, one may only consider the effective $g_\perp$ factor for $y_0=0$ in order to compare with the experimental measurements.

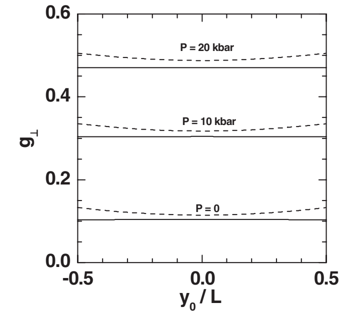

FIG. 3. Effective $g_\perp$ factor as a function of the orbit-center position for three different values of the applied hydrostatic pressure in a GaAs-$Ga_{0.7}Al_{0.3}As$ QW with $L_0=50$ Å. Solid and dashed lines correspond to $B=1$ T and $B=20$ T, respectively.

In Fig. 4, we have displayed the magnetic-field dependence of the electron effective $g_\perp$ factor in GaAs-$Ga_{0.7}Al_{0.3}As$ QWs with $L_0=50$ Å (solid lines) and $L_0=100$ Å (dashed lines) for three different values of the applied hydrostatic pressure and for the orbit-center position taken at the center of the wells. One may note that the effective Landé factor increases slightly and linearly as the magnetic field is increased, with slopes essentially independent of the well width. The increase in the effective $g_\perp$ factor is only of the order of 0.01 for the in-plane magnetic field changing from $B=5$ T to $B=20$ T. In contrast, the hydrostatic-pressure dependence of the effective $g_\perp$ factor is more remarkable [cf., Figs. 3–5]. The hydrostatic-pressure dependence of the electron $g_\perp$ factor in GaAs-$Ga_{0.7}Al_{0.3}As$ QWs is shown in Fig. 5 for various values of the QW width. Solid lines correspond to calculations performed for $B=1$ T and $y_0=0$, whereas dashed lines correspond to theoretical results obtained from Eq. (5), at $B=0$, for bulk GaAs and

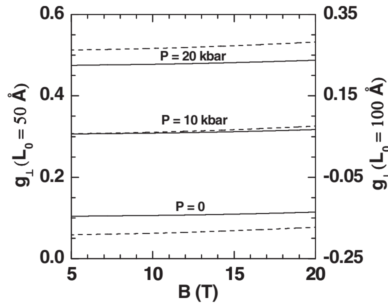

FIG. 4. Magnetic-field dependence of the effective $g_\perp$ factor in GaAs-$Ga_{0.7}Al_{0.3}As$ QWs for $P=0$, $P=10$ kbar, and $P=20$ kbar. Solid and dashed lines correspond to $L_0=50$ Å and $L_0=100$ Å, respectively. In all cases, the orbit-center position was taken at the center of the QW.

$Ga_{0.7}Al_{0.3}As$. The effective $g_\perp$ factor is an increasing function of the applied hydrostatic pressure, which is a consequence of the explicit hydrostatic-pressure dependence of the electron g factors corresponding to each building material of the QW. It is apparent from Fig. 5 that the applied hydrostatic pressure may be used in QWs, for instance, to tune[18] the Zeeman splitting in the limit of zero g factor. On the other hand, according to the present theoretical calculations, for all possible widths of the GaAs-$Ga_{0.7}Al_{0.3}As$ QW, the effective Landé factor is positive for hydrostatic pressures beyond 20 kbar (see the dashed curve for $L_0 \rightarrow \infty$ in Fig. 5). Thus, in addition, the applied hydrostatic pressure may be used to suppress the change on the sign of the effective $g_\perp$ factor as a function of the QW width.

Figure 6 displays the electron $g_\perp$ factor as a function of the L_0 GaAs-$Ga_{1-x}Al_xAs$ QW width for two different values of the aluminum concentration in the barriers. Calculations were carried out for $B=1$ T, orbit-center position at the center of the wells, and for different values of the hydrostatic pressure from $P=0$ to $P \simeq P_2$. Experimental data at $P=0$ are from Hannak *et al.*,[5] Le Jeune *et al.*,[6] Malinowski and Harley,[7] and Heberle *et al.*[8] The effective electron $g_\perp$ factor decreases as the well width is increased and changes its sign for the lowest values of the applied hydrostatic pressure. However, for $P > 20$ kbar, the $g_\perp$ factor remains positive in

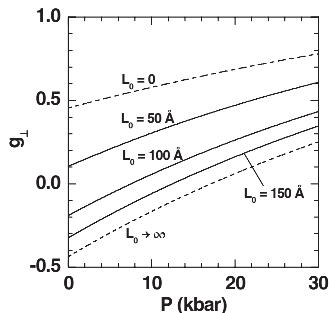

FIG. 5. Hydrostatic-pressure dependence of the electron $g_\perp$ factor in GaAs-$Ga_{0.7}Al_{0.3}As$ QWs for various values of the well width. Calculations were carried out for $B=1$ T and for the orbit-center position at the center of the wells. Dashed lines correspond to the numerical results obtained from Eq. (5) for bulk GaAs and $Ga_{0.7}Al_{0.3}As$ in the absence of the in-plane magnetic field.

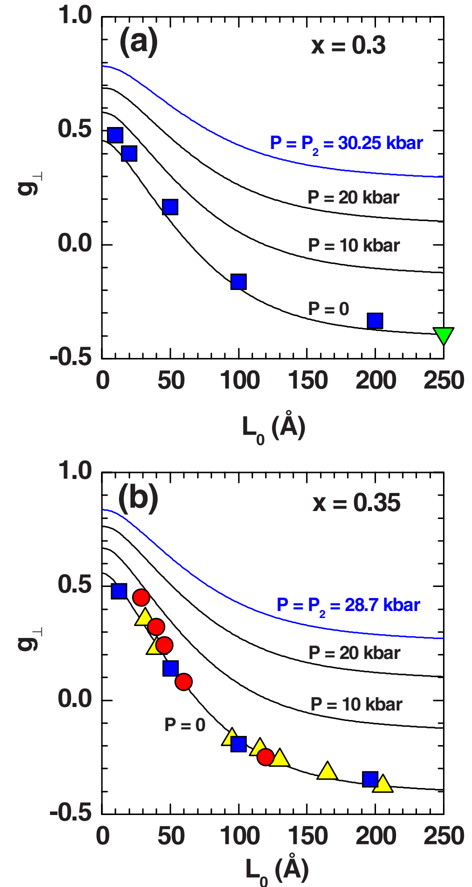

FIG. 6. (Color online) Electron $g_\perp$ factor, as a function of the well width, in (a) GaAs-$Ga_{0.7}Al_{0.3}As$ and (b) GaAs-$Ga_{0.65}Al_{0.35}As$ QWs for various values of the applied hydrostatic pressure. Theoretical results were obtained for $B=1$ T and for the orbit-center position at the center of the wells. Squares (Ref. 5), circles (Ref. 6), up triangles (Ref. 7), and down triangles (Ref. 8) correspond to experimental measurements at low values of applied magnetic fields and zero pressure.

the whole studied range of the GaAs-$Ga_{1-x}Al_xAs$ QW width. This behavior allows one to use the hydrostatic pressure to manipulate and tune the spin dynamics and spin relaxation in semiconductor QWs. Finally, in the absence of applied hydrostatic pressure, one may note the good agreement between the experimental measurements and present theoretical calculations for the two values of the aluminum concentration considered in the GaAs-$Ga_{1-x}Al_xAs$ QW barriers.

IV. CONCLUSIONS

Summing up, we have studied the effects of applied hydrostatic pressure and aluminum concentration on the effective Landé $g_\perp$ factor in semiconductor GaAs-$Ga_{1-x}Al_xAs$ QWs, under in-plane magnetic fields, by taking into account the nonparabolicity and anisotropy of the conduction band, as well as the hydrostatic-pressure and aluminum-concentration dependencies of the electron effective mass and Landé factor in each material forming the

GaAs-$Ga_{1-x}Al_xAs$ QW heterostructure. In this sense, we have first reviewed the properties of the g factor and electron effective mass in bulk GaAs and $Ga_{1-x}Al_xAs$ according to the $\mathbf{k}\cdot\mathbf{p}$ procedure, with model results fitted to give good agreement with available experimental measurements for the electron effective mass[31] and Landé factor.[2] The effective $g_\perp$ factor was studied as a function of the concentration x in the $Ga_{1-x}Al_xAs$ barrier, orbit-center position, applied magnetic field, hydrostatic pressure, and QW width. Theoretical calculations are found in excellent agreement with zero-pressure experimental measurements of the effective $g_\perp$ factor in GaAs-$Ga_{1-x}Al_xAs$ QWs. In addition, from the present results, we may conclude that it is possible to tune the effective $g_\perp$ factor by changing these parameters and therefore manipulate the spin dynamics and spin relaxation in GaAs-$Ga_{1-x}Al_xAs$ QWs.

ACKNOWLEDGMENTS

The authors would like to thank the Brazilian Agencies CNPq, FAPESP, MCT—Millenium Institute for Quantum Information, and MCT—Millenium Institute for Nanotechnology for partial financial support. This work was also partially financed by COLCIENCIAS and CODI—University of Antioquia. N.R. wishes to thank the warm hospitality of the Instituto de Física, Unicamp, Brazil, where part of this work was performed.

[1] C. Weisbuch and C. Hermann, Phys. Rev. B **15**, 816 (1977).
[2] C. Hermann and C. Weisbuch, Phys. Rev. B **15**, 823 (1977).
[3] M. Oestreich and W. W. Rühle, Phys. Rev. Lett. **74**, 2315 (1995).
[4] M. Oestreich, S. Hallstein, A. P. Heberle, K. Eberl, E. Bauser, and W. W. Rühle, Phys. Rev. B **53**, 7911 (1996).
[5] R. M. Hannak, M. Oestreich, A. P. Heberle, W. W. Ruhle, and K. Kohler, Solid State Commun. **93**, 313 (1995).
[6] P. Le Jeune, D. Robart, X. Marie, T. Amand, M. Brosseau, J. Barrau, V. Kalevcih, and D. Rodichev, Semicond. Sci. Technol. **12**, 380 (1997).
[7] A. Malinowski and R. T. Harley, Phys. Rev. B **62**, 2051 (2000).
[8] A. P. Heberle, W. W. Rühle, and K. Ploog, Phys. Rev. Lett. **72**, 3887 (1994).
[9] I. A. Yugova, A. Greilich, D. R. Yakovlev, A. A. Kiselev, M. Bayer, V. V. Petrov, Yu. K. Dolgikh, D. Reuter, and A. D. Wieck, Phys. Rev. B **75**, 245302 (2007).
[10] M. de Dios-Leyva, E. Reyes-Gómez, C. A. Perdomo-Leiva, and L. E. Oliveira, Phys. Rev. B **73**, 085316 (2006).
[11] M. de Dios-Leyva, N. Porras-Montenegro, H. S. Brandi, and L. E. Oliveira, J. Appl. Phys. **99**, 104303 (2006).
[12] A. A. Kiselev, E. L. Ivchenko, and U. Rössler, Phys. Rev. B **58**, 16353 (1998).
[13] T. P. Mayer Alegre, F. G. G. Hernández, A. L. C. Pereira, and G. Medeiros-Ribeiro, Phys. Rev. Lett. **97**, 236402 (2006).
[14] E. Reyes-Gómez, C. A. Perdomo-Leiva, M. de Dios-Leyva, and L. E. Oliveira, Phys. Rev. B **74**, 033314 (2006).
[15] Y. K. Kato, R. C. Myers, A. C. Gossard, and D. D. Awschalom, Science **306**, 1910 (2004).
[16] I. Zutic, J. Fabian, and S. Das Sarma, Rev. Mod. Phys. **76**, 323 (2004).
[17] Z. Chen, S. G. Carter, R. Bratschitsch, P. Dawson, and S. T. Cundiff, Nat. Phys. **3**, 265 (2007).
[18] D. R. Leadley, R. J. Nicholas, D. K. Maude, A. N. Utjuzh, J. C. Portal, J. J. Harris, and C. T. Foxon, Semicond. Sci. Technol. **13**, 671 (1998).
[19] C. Bosio, J. L. Staehli, M. Guzzi, G. Burri, and R. A. Logan, Phys. Rev. B **38**, 3263 (1988).
[20] H. M. Cheong, J. H. Burnett, W. Paul, P. F. Hopkins, K. Campman, and A. C. Gossard, Phys. Rev. B **53**, 10916 (1996).
[21] E. H. Li, Physica E (Amsterdam) **5**, 215 (2000).
[22] A. R. Goñi, K. Syassen, K. Strössner, and M. Cardona, Semicond. Sci. Technol. **4**, 246 (1989).
[23] M. Guzzi, E. Grilli, S. Oggioni, J. L. Staehli, C. Bosio, and L. Pavesi, Phys. Rev. B **45**, 10951 (1992).
[24] A. R. Goñi, K. Strössner, K. Syassen, and M. Cardona, Phys. Rev. B **36**, 1581 (1987).
[25] N. R. Ogg, Proc. Phys. Soc. London **89**, 431 (1966).
[26] B. O. McCombe, Phys. Rev. **181**, 1206 (1969).
[27] V. G. Golubev, V. I. Ivanov-Omskii, I. G. Minervin, A. V. Osutin, and D. G. Polyakov, Sov. Phys. JETP **61**, 1214 (1985).
[28] F. X. Bronold, I. Martin, A. Saxena, and D. L. Smith, Phys. Rev. B **66**, 233206 (2002).
[29] G. Dresselhaus, Phys. Rev. **100**, 580 (1955).
[30] E. Reyes-Gómez, N. Porras-Montenegro, C. A. Perdomo-Leiva, H. S. Brandi, and L. E. Oliveira (unpublished).
[31] M. Zachau, F. Koch, G. Weimann, and W. Schlapp, Phys. Rev. B **33**, 8564 (1986).
[32] A. M. Elabsy, J. Phys.: Condens. Matter **6**, 10025 (1994).
[33] J. H. Burnett, H. M. Cheong, W. Paul, E. S. Koteles, and B. Elman, Phys. Rev. B **47**, 1991 (1993).
[34] P. Y. Yu and M. Cardona, *Fundamentals of Semiconductors* (Springer-Verlag, Berlin, 1998).
[35] S. Adachi, J. Appl. Phys. **58**, R1 (1985).